IRSTI 29.19.16 https://doi.org/10.26577/RCPh97220263

K. Ganiyeva* , S. Karim , A. Abduvalov*
Nazarbayev University Research Administration, Astana, Kazakhstan
*e-mail: kamila.ganiyeva@nu.edu.kz, alshyn.abduvalov@nu.edu.kz

STUDY OF INTENSE PULSED ION BEAM IRRADIATION EFFECT ON MAGNETRON SPUTTERED ZNO THIN FILMS

ZnO thin films were fabricated via magnetron sputtering on FTO substrates and subsequently modified by different intense pulsed ion beam (IPIB) irradiations (5-20 A/cm^2) and 10 A/cm^2 with different pulse numbers (1, 3, and 6 pulses). IPIB treatment induces transformation of uniform nanograins into coarser, agglomerated, partially fused structures, and with a non-monotonic evolution of surface roughness. Despite these surface modifications, the ZnO films retain their hexagonal wurtzite crystal structure and have negligible changes in optical bandgap (~3.2 eV) that reveals the preservation of the bulk electronic structure. Additionally, irradiation alters the surface composition and introduces defect states, as reflected by changes in XPS in Zn/O ratio and increased interfacial heterogeneity. At moderate irradiation conditions, partial surface smoothing and structural relaxation occur, whereas higher fluence (multiple pulses) leads to significant defect accumulation. As a result, after testing photoactivity irradiated samples have increased interfacial charge-transfer resistance and reduced photocurrent density. Overall, IPIB irradiation predominantly modifies surface properties, and excessive defect formation under high fluence conditions deteriorates charge transport and photoelectrochemical performance.

Keywords: photocatalytic, magnetron, ZnO, intense pulsed ion beam, irradiation, thin films, water splitting, photoanode.

К.Г. Ганиева*, С. Карим, А.Ж. Абдувалов*
Nazarbayev University Research Administration, Астана, Қазақстан
*e-mail: kamila.ganiyeva@nu.edu.kz, alshyn.abduvalov@nu.edu.kz

Магнетрондық шандату әдісімен алынған ZnO жұқа қабықшаларына қарқынды импульстік иондық сәуле әсерін зерттеу

ZnO жұқа қабықшалары FTO төсемдерінде магнетрондық шаңдату әдісімен алынған және кейіннен әртүрлі қарқындылықтағы импульсті ион сәулесімен (IPIB) модификацияланды (5–20 А/см^2), сондай-ақ 10 А/см^2 кезінде әртүрлі импульс саны (1, 3 және 6) қолданылды. IPIB модификасиясы біркелкі нанотүйірлердің іріленген, агломерацияланған және ішінара бірігіп кеткен құрылымдарға айналуына әкеледі, бұл кезде бет кедір-бұдырлығының өзгерісі монотонды емес сипатта болады. Осы беткі өзгерістерге қарамастан, ZnO қабықтары гексагональды вюрциттік кристалдық құрылымын сақтайды және оптикалық тыйым салынған аймақтың ені (~3,2 эВ) айтарлықтай өзгермейді, бұл көлемдік электрондық құрылымның сақталғанын көрсетеді. Сонымен қатар, сәулелендіру бет құрамын өзгертеді және ақаулық күйлердің пайда болуына әкеледі, бұл XPS нәтижелерінде Zn/O қатынасының өзгеруі және интерфейстік біртексіздіктің артуы арқылы көрінді. Орташа сәулелендіру жағдайларында беттің ішінара тегістелуі және құрылымдық релаксация байқалады, ал жоғары флюенс (көп импульстар) айтарлықтай ақаулардың жиналуына алып келеді. Фотоактивтілікті сынау нәтижесінде сәулелендірілген үлгілерде интерфейстік заряд тасымалдау кедергісінің артуы және фототок тығыздығының төмендеуі байқалды. Жалпы алғанда, IPIB сәулелендіруі негізінен беткі қасиеттерді өзгертеді, ал жоғары флюенс жағдайында ақаулардың шамадан тыс түзілуі заряд тасымалдауды және фотоэлектрохимиялық қасиеттерді нашарлатады.

Түйін сөздер: фотокатализ, магнетрондық тозаңдату, ZnO, қарқынды импульсті ион сәулесі, сәулелендіру, жұқа қабықтар, суды ыдырату, фотоанод.

К.Г. Ганиева*, С. Карим, А.Ж. Абдувалов*
Nazarbayev University Research Administration, Астана, Казахстан
*e-mail: kamila.ganiyeva@nu.edu.kz, alshyn.abduvalov@nu.edu.kz

Исследование влияния облучения интенсивным импульсным ионным пучком на тонкие плёнки ZnO, полученные методом магнетронного распыления

Тонкие плёнки ZnO были получены методом магнетронного распыления на подложках FTO и затем модифицированы интенсивным импульсным ионным пучком (IPIB) при различных флюенсах (5–20 А/см^2), а также при 10 А/см^2 с разным числом импульсов (1, 3 и 6). IPIB модификация приводит к трансформации однородных нанозёрен в более крупные, агломерированные, частично сплавленные структуры, сопровождающейся немонотонным изменением шероховатости поверхности. Несмотря на эти изменения поверхности, плёнки ZnO сохраняют гексагональную кристаллическую структуру типа вюрцита, а изменения оптической ширины запрещённой зоны (~3,2 эВ) незначительны, что свидетельствует о сохранении электронной структуры. Кроме того, облучение изменяет состав поверхности и приводит к появлению дефектов, что отражается в данных XPS в виде изменения соотношения Zn/O и увеличения межфазной неоднородности. При умеренных условиях облучения наблюдаются частичное сглаживание поверхности и структурная релаксация, тогда как более высокий флюенс (многократные импульсы) приводит к значительному накоплению дефектов. В результате испытаний фотоактивности облучённые образцы демонстрируют увеличение межфазного сопротивления переносу заряда и снижение плотности фототока. В целом, облучение IPIB преимущественно модифицирует поверхностные свойства, а избыточное образование дефектов при высоких флюенсах ухудшает транспорт заряда и фотоэлектрохимические характеристики.

Ключевые слова: фотокатализ, магнетронное распыление, ZnO, интенсивный импульсный ионный пучок, облучение, тонкие плёнки, расщепление воды, фотоанод.

Introduction

Nowadays, fossil fuels such as coal, oil, and natural gas are the only available sources of energy with reasonable prices, yet their exploitation contributes significantly to climate change and environmental degradation [1,2]. In contrast, renewable energy sources, such as solar, wind, and water, offer sustainable alternatives. Among these, hydrogen has emerged as a promising clean fuel due to its high energy density, zero carbon emissions when produced from water, and versatility as an energy carrier for transportation, industry, and electricity generation [3–5]. Photoelectrochemical water splitting is one of the most promising methods to produce green hydrogen and oxygen utilizing solar energy [6–8]. The working principle of this method is centered in collecting the power of sunlight to promote the reaction, which takes place at the semiconductor-electrolyte interface [9,10]. Incident sunlight excites the semiconductor, creating electron-hole pairs. The generated charge carriers drive water oxidation at the anode and proton reduction at the cathode, producing hydrogen gas [11,12]. For efficient fuel conversion, the conduction band (CB) edge of a semiconductor must be positioned more negatively than the water reduction potential, while the valence band (VB) edge should be more positive than the water oxidation potential [13,14]. Although many semiconductors meet this thermodynamic requirement, in practice only a limited number, such as TiO_2, $SrTiO_3$, ZnO, and ZrO_2, possess suitably aligned CB and VB edges that make them suitable for photoelectrochemical water splitting applications [15,16]. ZnO is an n-type semiconductor that has a relatively wide bandgap of 3.36 eV, it is chemically stable [17,18], possesses good electron mobility of 210 $cm^2V^{-1}s^{-1}$, a high exciton binding energy of photogenerated electron-hole pairs, and it is non-toxic to the environment [19,20]. However, due to the wide band gap of ZnO photoanode, its photocatalytic efficiency can be improved by doping with C, N, Cu, Fe, doping with noble metal nanoparticles (NPs) as Ag NPs, AuNPs, Pd NPs, making composite with CdS, NiO, intense ion beam irradiation (IPIB) [21–24]. Among these methods, IPIB stands out as a unique technique that enables the modification of material surface with high-current density [25].

In our earlier works [26,27], IPIB irradiation has been successfully applied to enhance the photoactivity of WO_3 thin films. Both magnetron-sputtered and chemically deposited films exhibited distinct structural and morphological changes upon irradiation. After subsequent annealing, magnetron sputtered films had 80% PEC enhancement at 1.23 V vs RHE. Moreover, chemically deposited WO_3 films transformed into porous structures with increased thickness, resulting in higher absorbance and a 70 % enhancement in photocurrent density at 1.23 V vs. RHE compared with only annealed films. Although IPIB treatment reduced charge transport in spin-coated WO_3, the enhanced light-trapping and increased surface area maintained high photoactivity.

This work presents the ZnO thin films that were produced using the magnetron sputtering method with further IPIB irradiation by the INURA accelerator. Produced samples were analyzed for morphological, structural, optical, and PEC characteristics. It was revealed that irradiated samples showed decreased PEC performance with increasing IPIB current density from 5 to 20 A/cm^2 and with increased number of pulses (10 A/cm^2 3 and 6 pulses). Moreover, increasing current density and pulse number showed a significant morphological change where uniform nanograins become enlarged and agglomerated, fused (sintered), accompanied by localized thermal damage. There was no alteration in crystal structure of material and no change in the fundamental optical transparency upon irradiation.

Materials and Methods

Materials

FTO Glass substrates (OPVTech, FTO thickness 350 nm, glass thickness 2.2 mm, surface resistance <14.0 Ohms/sq). ZnO target was purchased from Kurt Lesker (2.00" Dia. x 0.125" Thick, 99.9% purity).

Sample fabrication

Commercial FTO Glass substrates were cleaned in DI water for 20 min and ethanol using ultrasonic bath for 15 min and placed in UV Ozone cleaner for 10 min to remove organic wastes and improve adhesion of the surface.

ZnO samples were prepared using RF magnetron sputtering technique. For that, samples were placed inside the chamber with Ar gas at pressure of 5 mTorr. Argon flow rate was 22.46 sccm. Other sputtering parameters: power - 30 W, deposition time - 45 min, substrate rotation rate - 2 rpm.

The IPIB treatment was conducted via the INURA accelerator at Nazarbayev University in Astana, Kazakhstan. This pulsed-power system is remarkably efficient, maintaining power consumption under 10 kW while achieving a peak power density of 10 MW/cm^2 at the target. Operating at 300-400 kV with a 10 kA beam current, the INURA delivers a 100 ns pulse (FWHM). This brief exposure induces an ultrafast annealing process, where the material undergoes intense heating in nanoseconds followed by microsecond-scale cooling.

ZnO samples were fabricated as non-irradiated and irradiated with different current densities such as 5 A/cm^2, 10 A/cm^2, 15 A/cm^2, 20 A/cm^2, 10 A/cm^2 3 pulses, and 10 A/cm^2 6 pulses.

Material characterization

Structural, morphological, optical properties were investigated using a Scanning electron microscope (SEM) by FIB/SEM Helios-5CX (Thermo Fisher), Rigaku Smart Lab Automated Multipurpose Grazing Incidence X-ray Diffractometer (GI-XRD) (Omega-0.5), UV-vis Infitek Double Beam UV Visible Spectrophotometer, SP-IUV8, SP-IUV9 (Infitek), X-ray Photoelectron Spectroscopy (XPS) with NEXSA (Thermo Scientific), and Atomic Force Microscope (AFM) with SmartSPM 1000 (Horiba).

PEC characterization

Linear sweep voltammetry (LSV) and electrochemical impedance spectroscopy (EIS) measurements were performed using a CHI660E potentiostat in a three-electrode configuration, with an Ag/AgCl reference electrode (3.5 M KCl) and a platinum counter electrode. ZnO non-irradiated and irradiated films were used as the working electrodes, and measurements were conducted in 0.16 M Na_2SO_4 electrolyte (pH 7.0). Photocurrent generation was measured under simulated solar illumination (PLS-FX300HU and PLS-EM solar simulators, AM 1.5, 100 mW/cm^2), with all potentials converted to the reversible hydrogen electrode (RHE) scale:

$$V_{RHE} = V_{Ag/AgCl} + 0.059 \times pH + 0.205 \quad (1)$$

where, $V_{Ag/AgCl}$ is the applied potential and 0.205 is the standard potential for the Ag/AgCl, KCl (3.5 M) reference electrode.

Electrochemical impedance spectroscopy (EIS) measurements were carried out under illumination at a DC bias of 0.68 V vs. RHE, using an AC perturbation amplitude of 50 mV over a frequency range from 1 Hz to 10 kHz and the impedance data were analyzed using EIS Spectrum Analyzer software.

Results and discussion

The SEM images presented in Figure 1 reveal a clear evolution of surface morphology of ZnO films as a function of irradiation current density and pulse number. The non-irradiated reference sample (Figure 1a) has a uniform and compact surface composed of closely packed ZnO nanograins and low porosity, indicating a homogeneous polycrystalline nanostructure. Upon irradiation at 5 A/cm^2 (Figure 1b), the grains become slightly more distinct and better defined, and mild grain growth while the film remains dense and continuous. At 10 A/cm^2 (Figure 1c) localized melting effects are observed that result in a more compact and uniform morphology. Further increasing the current density to 15 A/cm^2 (Figure 1d) leads to the formation of ZnO agglomerates. The surrounding grains appear more fused with a thermally induced sintering. At 20 A/cm^2 (Figure 1e), the surface regains a comparatively uniform texture, the grains are slightly coarser than in the lower-current samples, but the surface becomes more homogeneous with possible reorganization at higher irradiation.

When multiple pulses are applied at 10 A/cm^2, the morphological changes become more severe. After 3 pulses (f), the surface undergoes severe restructuring, characterized by agglomerated clusters surrounded by uniformly packed nanograins. There are large irregular aggregates that appear with excessive energy accumulation and enhanced particle coalescence. With 6 pulses (g), morphology becomes more stabilized compared to the 3-pulse condition. Although agglomeration is still present, the distribution of particles appears more uniform, and the film has partial continuity.

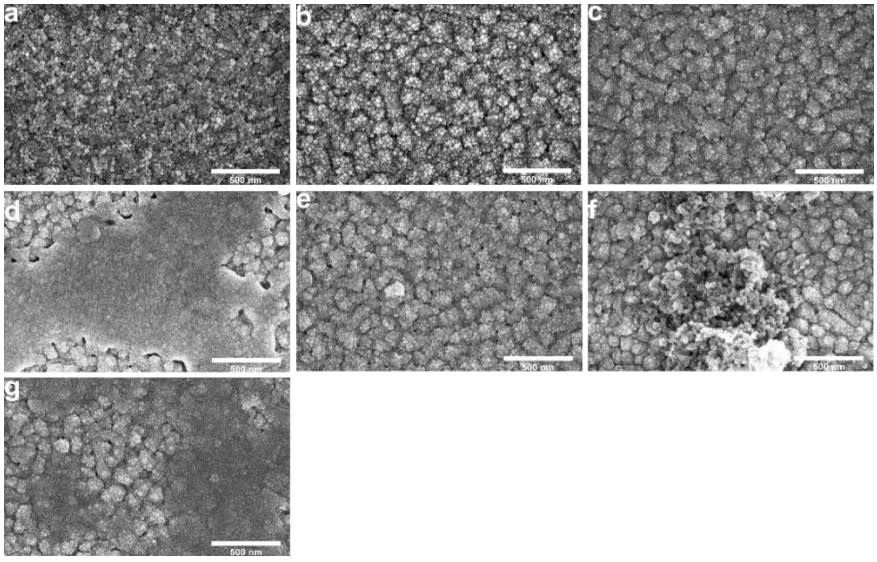

Figure 1 - SEM of ZnO samples: a) Ref, b) 5 A/cm^2, c) 10 A/cm^2, d) 15 A/cm^2, e) 20 A/cm^2, f) 10 A/cm^2 3 pulses, g) 10 A/cm^2 6 pulses under 200k magnification

The UV-vis absorption spectra in Figure 2 of the ZnO films subjected to pulsed proton-beam irradiation show only subtle but systematic changes with increasing ion-beam current density and pulse number. In the first series (5-20 A/cm^2, one pulse), the overall spectral shape remains nearly identical to the reference sample, with only a slight increase in absorption in the near-band-edge region (370-420 nm) that suggests a very modest rise in sub-gap or tail-state density, while the visible-range background (450-700 nm) remains essentially unchanged indicating that no strong defect-related coloration or deep-level absorption was introduced by single-pulse irradiation. In the second series with increased pulse number (at 10 A/cm^2, 1, 3, and 6 pulses), the trend becomes more pronounced: additional pulses cause a gradual upward shift in the absorption edge region (arrow), consistent with cumulative generation of shallow defect states (likely oxygen vacancies or surface disorder) or a slight increase in light scattering due to surface roughening. The absence of a pronounced red shift and visible-range absorption indicates that the irradiation does not create deep mid-gap states nor induce any major structural or chemical transformation, aligning with the XRD results (coming next) that show preserved crystallinity. Overall, the data shows that nanosecond proton irradiation produces only mild, pulse-accumulating modifications near the ZnO absorption edge without altering the fundamental optical transparency of the films.

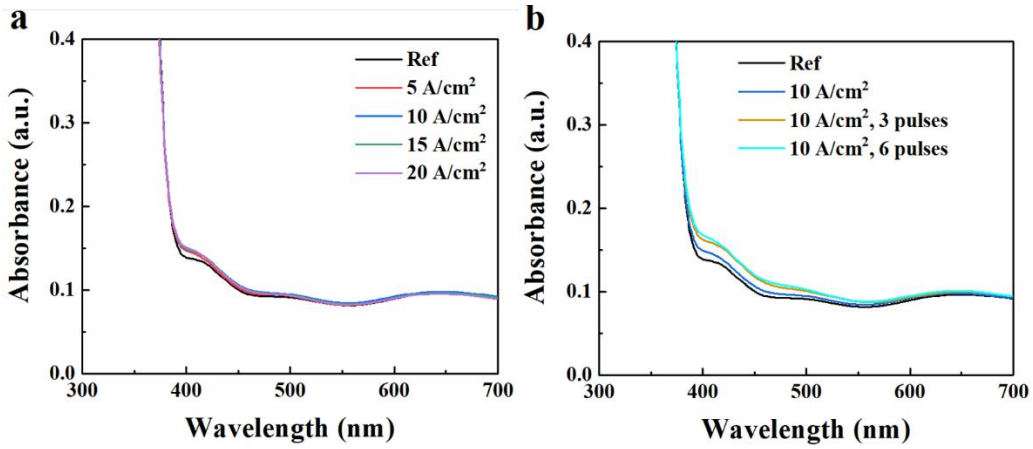

Figure 2 - UV-vis spectra of ZnO samples after irradiation: a) by increasing ion beam current density and b) by increasing pulse numbers

The optical bandgap of the ZnO thin films was determined using Tauc plot in Figure 3 for a direct allowed transition by plotting $\alpha h\nu^2$ as a function of photon energy. The bandgap values were obtained by extrapolating the linear region near the absorption edge to $\alpha h\nu^2 = 0$. Figure 3 shows that all samples have bandgap energies of approximately 3.2 eV; therefore, IPIB irradiation does not significantly change the intrinsic electronic structure of ZnO.

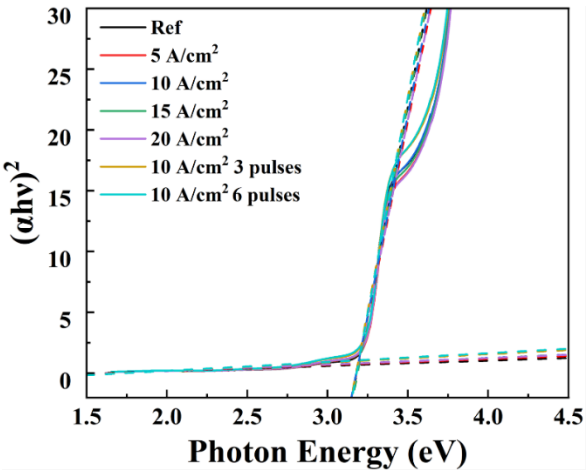

Figure 3 - Tauc plots of ZnO samples

The GI-XRD patterns of the ZnO film and the IPIB-treated ZnO film in Figure 4 show the characteristic spectra of hexagonal wurtzite ZnO, matching PDF-2 card 00-003-0888. The dominant ZnO peaks (100), (002), (101), and (102) are clearly visible at their expected 2θ positions, and no systematic shifts, broadening, or intensity changes are observed after irradiation, indicating that the nanosecond high-current proton beam did not alter the long-range crystallinity or induce detectable strain or phase transformation.

Several additional peaks appear in the region between 37-39° and near 48-50°, but they do not correspond to any strong or medium-intensity ZnO peaks in the standard card. Overall, the ZnO structure appears unchanged by irradiation, and additional peaks outside the main ZnO peaks remain uncertain in origin and cannot be conclusively assigned.

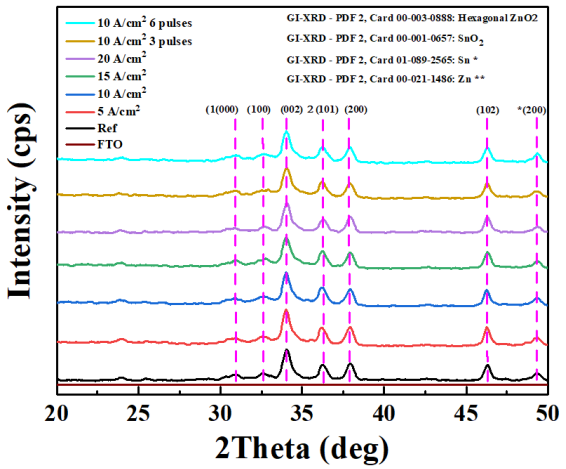

Figure 4 - GI-XRD patterns of ZnO samples before and after irradiation

Electrochemical impedance spectroscopy (EIS) was used to evaluate the effect of IPIB irradiation on the electrical and interfacial properties of ZnO thin films. The impedance spectra that is shown in Figure 5 were fitted using an equivalent circuit consisting of a solution resistance (R_s), a constant phase element (CPE), and a polarization resistance (R_p). EIS fitted values are presented in Table 1.

The series resistance (R_s) remains nearly constant for most samples (~40-46 Ω) and differences in contact resistance and electrolyte conductivity are negligible. Only the samples that undergone the pulsed regime treatment (10 A/cm², 3 and 6 pulses) show slightly higher R_s values (~57-61 Ω) that are

related to the increased structural disorder; however, the dominant changes arise from the electrode/electrolyte interface.

The most significant variation is observed in the polarization resistance (R_p), which reflects the charge-transfer resistance where higher R_p values show high resistance and high recombination rates and lower photocurrent; however lower R_p indicates more efficient interfacial charge transfer and decreased recombination losses. Among all samples, the reference ZnO film has the lowest R_p (~8.91 kΩ) and the most favorable charge-transfer conditions. Upon irradiation at 5-10 A/cm^2, R_p increases to ~10.7-11.0 kΩ because there is a defect formation and surface disorder that hinder charge transfer. The effect becomes more pronounced in the treatment with 10 A/cm^2 3 and 6 pulses, where R_p reaches its maximum values (~13.2 kΩ for 3 pulses and ~15.0 kΩ for 6 pulses). These samples have severe recombination and interfacial degradation due to accumulated defects. At IPIB irradiation of 15-20 A/cm^2, R_p decreases again (~9.3-9.9 kΩ) because of the partial recovery of charge transport, possibly due to defect recombination or structural relaxation. The capacitive behavior of the ZnO/electrolyte interface is described by the constant phase element (CPE), where CPE-T represents the effective interfacial capacitance and CPE-P (n) indicates deviation from ideal capacitive behavior. The reference sample shows relatively low CPE-T (~5.05×10^{-6}), but after irradiation, CPE-T increases significantly, reaching maximum values in the 3 and 6 pulsed samples (~13.83-15.4×10^{-6}), which enhances surface area and increases density of defect states. CPE-P decreases from ~0.79 (reference) to ~0.67-0.69 (3 and 6 pulsed samples) that means the increased surface heterogeneity and a broader distribution of charge-transfer paths. For IPIB of 15-20 A/cm^2, CPE-T decreases and CPE-P slightly increases (~0.73-0.75) which points to partial restoration of interfacial uniformity. Overall, the combination of increasing R_p, higher CPE-T, and lower CPE-P with irradiation confirms that IPIB treatment introduces surface defects and disorder that degrade interfacial charge-transfer efficiency, with the strongest effect observed under multiple-pulse conditions.

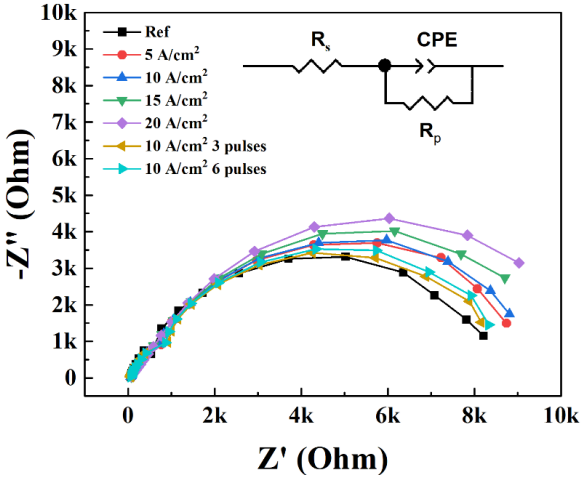

Figure 5 - EIS of irradiated and non-irradiated ZnO samples

Table 1. EIS fitting results of all samples

Sample	R_s	CPE-T (×10^{-6})	CPE-P (×10^{-3})	R_p
Ref	45.68±2.54	5.05±0.25	795.80±6.8	8913±203.70
5 A/cm^2	42.04±6.07	8.67±0.80	721±13.09	10725±612.60
10 A/cm^2	42.73±6.03	8.67±0.75	716.64±12.46	11044±607.69
10 A/cm^2 3 pulses	60.93±7.14	13.83±1.37	694.22±15.14	13229±1152
10 A/cm^2 6 pulses	57.68±8.89	15.44±1.79	677.28±17.79	15043±1782.70
15 A/cm^2	41.04±6.91	7.00±0.86	752.60±17.35	9325±590.37
20 A/cm^2	40.62±5.97	7.73±0.75	734.84±13.69	9890±533.16

The PEC LSV measurements in Figure 6 reveal a clear and systematic decline in chopped photocurrent density as the ion beam irradiation current density increases. In the first series (one pulse, 5-20 A/cm^2), all irradiated ZnO films have noticeably lower photocurrent compared to the pristine reference, with the suppression becoming stronger at higher irradiation currents indicating that even a single 100-ns high-current pulse introduces defect states or surface disorder that hinder charge separation or increase recombination. In the second series (at 10 A/cm^2 with 1, 3, and 6 pulses), the photocurrent decreases progressively with additional pulses that correspond to a cumulative degradation effect. Overall, PEC results show that IPIB irradiation deteriorates photoelectrochemical activity of ZnO. Also, there is an alteration on surface/interface electronic properties rather than on structural and bandgap. However, the onset potential and the bulk band structure do not change.

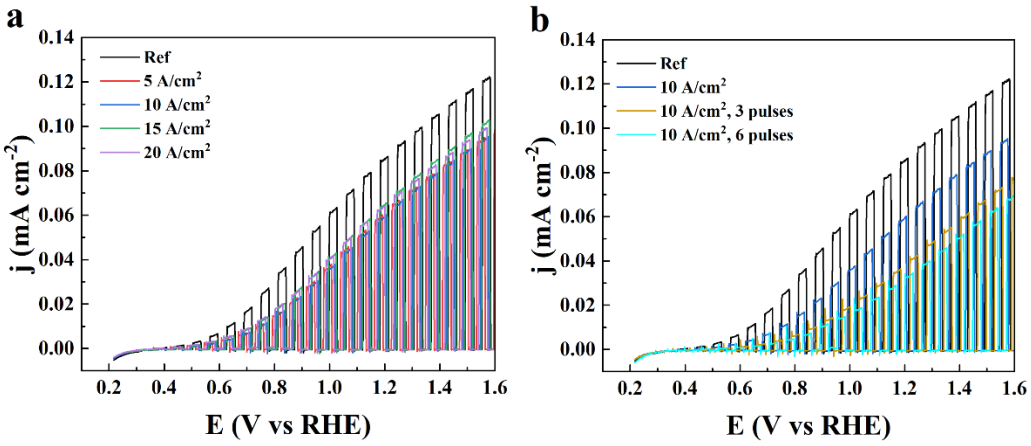

Figure 6 - PEC LSV curves of ZnO samples after irradiation: a) by increasing ion beam current density and b) by increasing pulse numbers

The XPS quantitative analysis in Figure 7 and Table 2 reveals a strong dependence of surface composition on IPIB current density and pulse number. The reference ZnO sample has a Zn/O atomic ratio of 0.39 (Zn 2p is 27.80 at.%, O 1s is 72.20 at.%), indicating an oxygen-rich surface compared to the ideal stoichiometric value of 1.0 expected for ZnO. Upon treatment at 5 A/cm^2, the Zn 2p content increases to 32.72 at.% and the Zn/O ratio rises to 0.49, that is a partial reduction of surface oxygen species. In contrast, treatment at 10 A/cm^2 results in a significant oxygen enrichment (O 1s is 80.57 at.%) and a decreased Zn/O ratio of 0.24 that demonstrates enhanced surface oxidation or adsorption of oxygen-containing species. At 15 A/cm^2 and 20 A/cm^2, the Zn/O ratios (0.39 and 0.35, respectively) remain below unity, still reflecting oxygen-rich surfaces. A pronounced deviation is observed for the 10 A/cm^2 sample subjected to 3 pulses, where Zn 2p dramatically increases to 65.80 at.% and oxygen decreases to 34.20 at.%, yielding a Zn/O ratio of 1.92. However, increasing the pulse number to 6 at the same current density restores a more balanced composition (Zn/O ≈ 0.48), comparable to the 5 A/cm^2 condition. Overall, the results demonstrate that both IPIB current density and pulse regime critically influence surface stoichiometry, where all of the samples have oxygen-rich surfaces except 10 A/cm^2 3 pulses that shows the highest Zn 2p at.% among all samples and Zn/O ratio closer to sub-stoichiometric (1.92) conditions.

Table 2. Elemental composition (at.%) and Zn/O ratio

Element	Ref	5 A/cm^2	10 A/cm^2	15 A/cm^2	20 A/cm^2	10 A/cm^2, 3 pulses	10 A/cm^2, 6 pulses
Zn 2p (at.%)	27.80	32.72	19.43	28.11	26.11	65.80	32.59
O 1s (at.%)	72.20	67.28	80.57	71.89	73.89	34.20	67.41
Zn/O Ratio	0.39	0.49	0.24	0.39	0.35	1.92	0.48

Atomic Force Microscopy (AFM) that is presented in Figure 8 was used to investigate surface morphology of ZnO thin films before and after IPIB irradiation. Bare FTO substrate has a granular morphology and a relatively high surface roughness with an average surface roughness S_a of 9.29±0.23 nm and RMS roughness S_q of 11.46±0.23 nm. After the deposition of ZnO (ref sample) the surface becomes smoother with S_a and S_q values of 7.39±0.68 nm and 9.11±0.71 nm respectively. After irradiation with 5 A/cm^2 the surface roughness increases S_a is 8.17±2.22 nm and S_q is 10.12±2.15 nm that is attributed to the formation of non-uniform packed structures. However, at 10-20 A/cm^2 IPIB irradiation the roughness S_a decreases to 5.46±0.20 nm (10 A/cm^2) and to 5.8±0.18 nm and 5.8±0.63 nm (15-20 A/cm^2). It suggests the formation of more compact and homogeneous ZnO thin films. Also, pulsed regimes have improvements in the surface smoothness. 3 pulses have the lowest roughness with S_a of 5.04±0.49 nm and S_q of 6.32±0.68 nm, 6 pulses have slightly increased S_a value of 5.29±0.27 nm and S_q of 6.54±0.21 nm. Figure 9 illustrates the 3D AFM images that correlate with these findings and show a transition from irregular, coarse grains to more uniform and densely packed nanostructures.

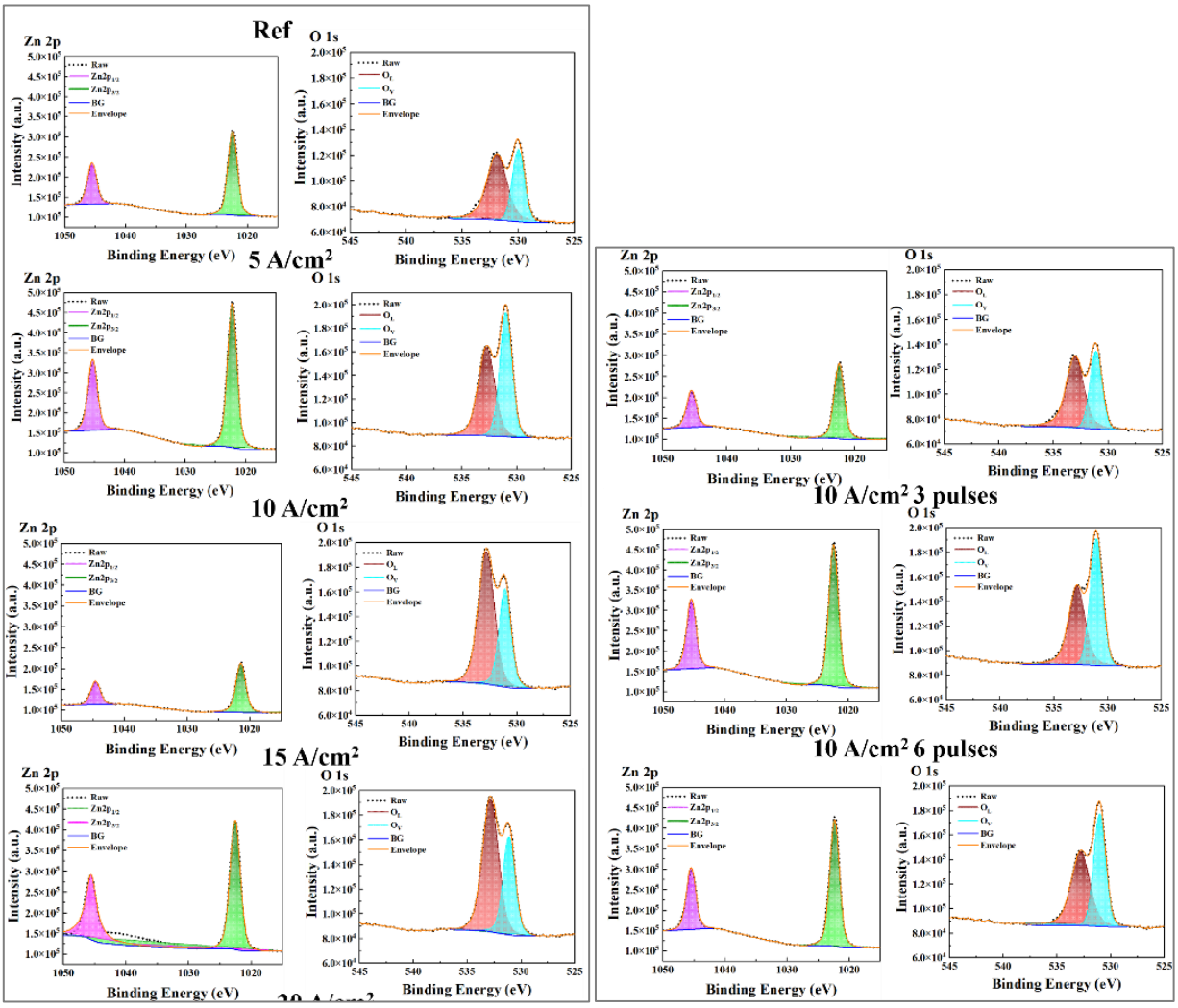

Figure 7 - XPS spectra of ZnO samples

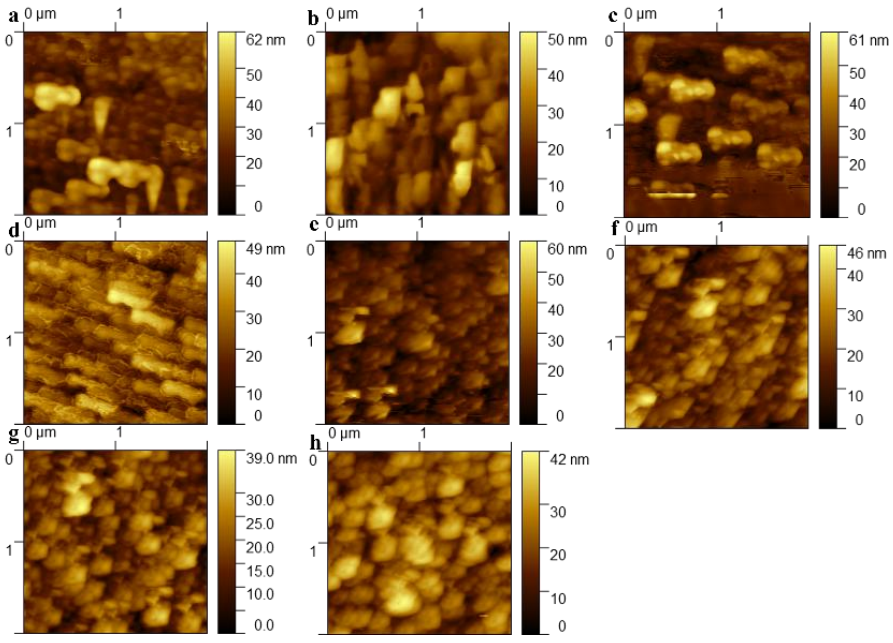

Figure 8 - AFM images of ZnO samples: a) FTO substrate, b) ref, c) 5 A/cm^2, d) 10 A/cm^2, e) 15 A/cm^2, f) 20 A/cm^2, g) 10 A/cm^2 3 pulses, h) 10 A/cm^2 6 pulses

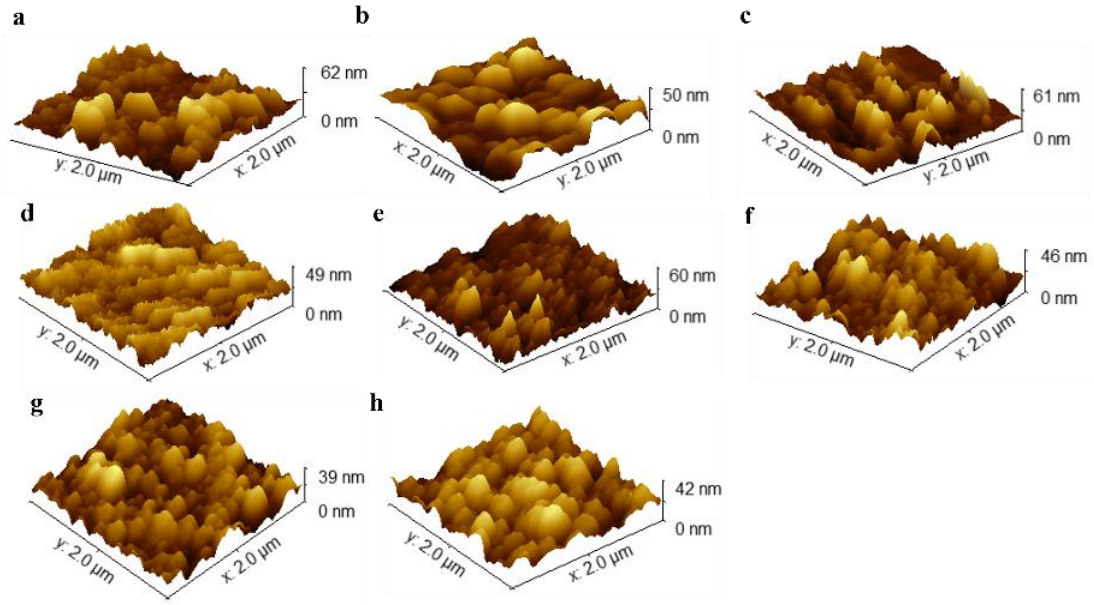

Figure 9 - 3D AFM images of ZnO samples: a) FTO substrate, b) ref, c) 5 A/cm^2, d) 10 A/cm^2, e) 15 A/cm^2, f) 20 A/cm^2, g) 10 A/cm^2 3 pulses, h) 10 A/cm^2 6 pulses

Table 3. AFM roughness parameters

Sample	S_a, nm	S_q, nm
FTO	9.29±0.23	11.46±0.30
Ref	7.39±0.68	9.11±0.71
5 A/cm^2	8.17±2.22	10.12±2.15
10 A/cm^2	5.46±0.20	6.85±0.46
15 A/cm^2	5.8±0.18	7.57±0.39
20 A/cm^2	5.8±0.63	7.28±0.67
10 A/cm^2 3 pulses	5.04±0.49	6.32±0.68
10 A/cm^2 6 pulses	5.29±0.27	6.54±0.21

Conclusion

Overall, increasing fluence (more pulses at the same energy) has a stronger influence on ZnO because defects accumulate with each pulse, the optical edge is degraded and photocurrent is reduced. Increasing energy per pulse (higher current density) causes an instant drop in PEC performance, but the effect is limited to the damage created in a single 100-ns pulse. In contrast, additional pulses create new recombination centers and surface disorder. XRD shows no structural changes in either case, meaning the differences arise from defect buildup energy controls the severity per pulse, while fluence controls the total defect dose. Fluence therefore dominates the overall degradation of ZnO electronic and photoelectrochemical properties.

The effect of intense pulsed ion beam irradiation on magnetron-sputtered ZnO thin films was systematically investigated in terms of structural, optical, morphological, and photoelectrochemical properties. SEM and AFM analyses revealed that increasing ion beam current density and pulse number leads to significant surface modification, including grain growth, agglomeration, and localized thermal damage. However, GI-XRD results illustrate that the hexagonal wurtzite crystal structure of ZnO remains unchanged after irradiation. It suggests that irradiation primarily affects the surface morphology rather than the bulk crystal lattice.

UV-vis spectroscopy showed only minor variations in absorption and no significant change in the optical bandgap (~3.2 eV), suggesting that the fundamental electronic structure of ZnO remains largely unaffected. In contrast, according to the XPS analysis surface composition and Zn/O ratio are changed because of irradiation modifications of surface stoichiometry.

EIS revealed increased polarization resistance R_p and interfacial disorder in irradiated samples,

particularly for multiple-pulse treatments, which is an indication of hindered charge transfer processes at the ZnO/electrolyte interface. Consistent with these findings, PEC measurements showed a systematic decrease in photocurrent density with increasing irradiation current density and pulse number.

Overall, the results demonstrate that while IPIB irradiation does not significantly alter the crystal structure or optical bandgap of ZnO, it strongly affects surface morphology, defect density, and interfacial charge transfer properties. Defect accumulation formed at increasing irradiation fluence (number of pulses), which leads to enhanced recombination, reduced carrier transport efficiency and decreased PEC performance.

Acknowledgments

This research was funded by the Science Committee of the Ministry of Science and Higher Education of the Republic of Kazakhstan (Grant No. BR28712489).

Author Contributions

K.G. Ganiyeva: Writing - Original Draft, Visualization, Software, Investigation, Formal Analysis. **S. Karim:** Methodology, Investigation, Formal Analysis. **A.Zh. Abduvalov:** Writing - Review & Editing, Methodology, Data Curation, Validation, Conceptualization.

References

1. A. G. Olabi and M. A. Abdelkareem, Renewable energy and climate change, *Renew. Sustain. Energy Rev.* **158**, (2022). https://doi.org/10.1016/j.rser.2022.112111
2. M. Riffat, H. Ali, H. A. Qayyum, M. Bilal, and T. Hussain, Enhanced solar-driven water splitting by ZnO/CdTe heterostructure thin films-based photocatalysts, *Int. J. Hydrogen Energy* **48**, 22069 (2023). https://doi.org/10.1016/j.ijhydene.2023.03.068
3. S. Ye, C. Ding, M. Liu, A. Wang, Q. Huang, and C. Li, Water oxidation catalysts for artificial photosynthesis, *Adv. Mater.*, (2019). https://doi.org/10.1002/adma.201902069
4. C. Zou et al., Industrial status, technological progress, challenges, and prospects of hydrogen energy, *Nat. Gas. Ind. B* **9**, 427-447 (2022). https://doi.org/10.1016/j.ngib.2022.04.006
5. S. Evro, B. A. Oni, and O. S. Tomomewo, Carbon neutrality and hydrogen energy systems, *Int. J. Hydrogen Energy* **78**, 1449-1467 (2024). https://doi.org/10.1016/j.ijhydene.2024.06.407
6. N. Sazali, Emerging technologies by hydrogen: A review, *Int. J. Hydrogen Energy* **45**(38), 18753-18771 (2020). https://doi.org/10.1016/j.ijhydene.2020.05.021
7. M. Kumar, B. Meena, P. Subramanyam, D. Suryakala, and C. Subrahmanyam, Recent trends in photoelectrochemical water splitting: The role of cocatalysts, *NPG Asia Mater.* **14**(1), 88 (2022). https://doi.org/10.1038/s41427-022-00436-x
8. F. Qureshi and M. Tahir, Photoelectrochemical water splitting with engineering aspects for hydrogen production: Recent advances, strategies and challenges, *Int. J. Hydrogen Energy*, **69**, 760-776 (2024). https://doi.org/10.1016/j.ijhydene.2024.05.039
9. M. Siahsahlan, S. Mohammadi Aref, and H. Naghshara, Structural and optical properties of ZnO thin films as a function of pH value and its effect on photoelectrochemical water splitting, *Phys. Scr.* **99**(5), (2024). https://doi.org/10.1088/1402-4896/ad3689
10. A. Vilanova, P. Dias, T. Lopes, and A. Mendes, The route for commercial photoelectrochemical water splitting: A review of large-area devices and key upscaling challenges, *Chem. Soc. Rev.* **53**, 2388-2434 (2024). https://doi.org/10.1039/D1CS01069G
11. G. Liu, Y. Xu, T. Yang, and L. Jiang, Recent advances in electrocatalysts for seawater splitting, *Nano Mater. Sci.* **5**, 101-116 (2023). https://doi.org/10.1016/j.nanoms.2020.12.003
12. W. Wang, M. Xu, X. Xu, W. Zhou, and Z. Shao, Perovskite Oxide Based Electrodes for High-Performance Photoelectrochemical Water Splitting, *Angew. Chem. Int. Ed.* **59**(1), 136-152 (2020). https://doi.org/10.1002%2Fanie.201900292
13. L. Kavan, Electrochemistry and band structure of semiconductors (TiO_2, SnO_2, ZnO): Avoiding pitfalls and textbook errors, *J. Solid State Electrochem.* **28**, 829-845 (2024). https://doi.org/10.1007/s10008-023-05770-w
14. A. Hezam, Q. A. Drmosh, D. Ponnamma, M. A. Bajiri, M. Qamar, K. Namratha, M. Zare, M. B. Nayan, S. A. Onaizi, and K. Byrappa, Strategies to enhance ZnO photocatalyst's performance for water treatment: A comprehensive review, *Chem. Rec.* **22**, e202100299 (2022). https://doi.org/10.1002/tcr.202100299
15. P. Subramanyam, B. Meena, V. Biju, H. Misawa, and S. Challapalli, Emerging materials for plasmon-assisted photoelectrochemical water splitting, *J. Photochem. Photobiol., C.* **51**, 100472 (2022). https://doi.org/10.1016/j.jphotochemrev.2021.100472
16. Y. Qiu, Z. Pan, H. Chen, D. Ye, L. Guo, Z. Fan, and S. Yang, Current progress in developing metal oxide nanoarrays-based photoanodes for photoelectrochemical water splitting, *Sci. Bull.* **64**(18), 1348-1380 (2019). https://doi.org/10.1016/j.scib.2019.07.017

17. L. Liccardo, E. Lushaj, L. Dal Compare, E. Moretti, and A. Vomiero, Nanoscale ZnO/α-Fe_2O_3 heterostructures: Toward efficient and low-cost photoanodes for water splitting, *Small Sci.* **2**(3), 2100104 (2022). https://doi.org/10.1002/smsc.202100104

18. E. B. Buzok, S. Yalcin, G. Demircan, D. Yılmaz, B. Aktas, and E. Aytar, The structural, optical, electrical and radiation shielding properties of Co-doped ZnO thin films, *Radiat. Phys. Chem.* **222**, 111840 (2024). https://doi.org/10.1016/j.radphyschem.2024.111840

19. M. Zayed, N. Nasser, M. Shaban, H. Alshaikh, H. Hamdy, and A. M. Ahmed, Effect of morphology and plasmonic on Au/ZnO films for efficient photoelectrochemical water splitting, *Nanomater*. **11**(9), 2338 (2021). https://doi.org/10.3390/nano11092338

20. Z. Kang, H. Si, S. Zhang, J. Wu, Y. Sun, Q. Liao, Z. Zhang, and Y. Zhang, Interface engineering for modulation of charge carrier behavior in ZnO photoelectrochemical water splitting, *Adv. Funct. Mater.* **29**(15). https://doi.org/10.1002/adfm.201808032

21. Y. Sun, W. Zhang, Q. Li, H. Liu, and X. Wang, Preparations and applications of zinc oxide based photocatalytic materials, *Adv. Sens. Energy Mat.*, **2**(3), 100069 (2023). https://doi.org/10.1016/j.asems.2023.100069

22. L. Dejam, S. Kulesza, J. Sabbaghzadeh, A. Ghaderi, S. Solaymani, Ștefan Țălu, M. Bramowicz, M. Amouamouha, A. hossein S. shayegan, and A. hossein Sari, ZnO, Cu-doped ZnO, Al-doped ZnO and Cu-Al doped ZnO thin films: Advanced micro-morphology, crystalline structures and optical properties, *Results Phys.* **44**, 106209 (2023). https://doi.org/10.1016/j.rinp.2023.106209

23. H. Lu, Y. Liu, S. Zhang, J. Wan, X. Wang, L. Deng, J. Kan, and G. Wu, Clustered tubular S-scheme ZnO/CdS heterojunctions for enhanced photocatalytic hydrogen production, Mater. Sci. Eng. B **289**, 116282 (2023). https://doi.org/10.1016/j.mseb.2023.116282

24. H. A. Mustafa, S. M. Hamad, and D. A. Jameel, Design and characterization of ZnO/NiO and ZnO/CuO heterostructures for high-performance solar cell applications, *Discov. Electron.* **3**(37), (2026). https://doi.org/10.1007/s44291-026-00188-w

25. V. Kumar, J. Prakash, D. Pathak, D. P. Sharma, L. P. Purohit, and H. C. Swart, Ion beam engineering of implanted ZnO thin films for solar cell and lighting applications, *Chem. Eng. J. Adv.* **15**, 100501 (2023). https://doi.org/10.1016/j.ceja.2023.100501

26. A. Abduvalov, M. Kaikanov, T. S. Atabaev, and A. Tikhonov, Improving photoelectrochemical activity of magnetron-sputtered double-layer tungsten trioxide photoanodes by irradiation with intense pulsed ion beams, *Nanomater*. **12**(15), 2639 (2022). https://doi.org/10.3390/nano12152639

27. A. Abduvalov, A. Kemelbay, K. Baigarin, M. S. Kiani, T. S. Atabaev, and M. Kaikanov, Creation of light trapping structures on spin-coated PVA containing WO_3 photo anodes by intense pulsed ion beam irradiation and their photocatalytic studies, *Appl. Surf. Sci.* **709**, 163874 (2025). https://doi.org/10.1016/j.apsusc.2025.163874

Information about authors:

Kamila Ganiyeva (corresponding author) – MSc in Chemistry, research assistant, Nazarbayev University Research Administration, (Astana, Kazakhstan, e-mail: kamila.ganiyeva@nu.edu.kz).

Sumera Karim – PhD Candidate in Physics, research assistant, Nazarbayev University Research Administration, (Astana, Kazakhstan, e-mail: sumera.karim@nu.edu.kz).

Alshyn, Abduvalov (corresponding author) – PhD in Physics, Nazarbayev University Research Administration, (Astana, Kazakhstan, e-mail: alshyn.abduvalov@nu.edu.kz).

Авторлар туралы мәлімет:

Камила Ганиева (автор-корреспондент) – химия ғылымдарының магистрі, зерттеуші-ассистент, Nazarbayev University Research Administration, (Астана, Қазақстан, e-mail: kamila.ganiyeva@nu.edu.kz).

Сумера Карим, физика саласындағы PhD докторанты, зерттеуші-ассистент, Nazarbayev University Research Administration, (Астана, Қазақстан, e-mail: sumera.karim@nu.edu.kz)ю

Алшын Абдувалов (автор-корреспондент) – Физика бойынша PhD, Nazarbayev University Research Administration, (Астана, Қазақстан, e-mail: alshyn.abduvalov@nu.edu.kz).

Сведения об авторах:

Камила Ганиева (автор-корреспондент) – магистр наук в химии, научный ассистент, Nazarbayev University Research Administration, (Астана, Казахстан, e-mail: kamila.ganiyeva@nu.edu.kz).

Сумера Карим, соискатель степени PhD по физике, научный ассистент, Nazarbayev University Research Administration, (Астана, Казахстан, e-mail: sumera.karim@nu.edu.kz).

Алшын Абдувалов (автор-корреспондент) – PhD по физике, Nazarbayev University Research Administration, (Астана, Казахстан, e-mail: alshyn.abduvalov@nu.edu.kz).

Article history: *received: 23 April 2026; accepted: 28 July 2026.*
Мақала тарихы: *түсті: 23 сәуір 2026; қабылданды: 28 шілде 2026.*
История статьи: *поступила: 23 апреля 2026; принята: 28 июля 2026.*